DISCRETE AND CONTINUOUS
DYNAMICAL SYSTEMS–SERIES B
Volume **4**, Number **1**, February **2004**

Website: http://AIMsciences.org

pp. **39–58**

A MATHEMATICAL MODEL OF TUMOR-IMMUNE EVASION AND siRNA TREATMENT

J.C. Arciero

Department of Mathematics
University of Michigan
Ann Arbor, Michigan

T.L. Jackson

Department of Mathematics
University of Michigan
Ann Arbor, Michigan

D.E. Kirschner

Department of Microbiology and Immunology
University of Michigan
Ann Arbor, Michigan

Abstract. In this paper a mathematical model is presented that describes growth, immune escape, and siRNA treatment of tumors. The model consists of a system of nonlinear, ordinary differential equations describing tumor cells and immune effectors, as well as the immuno-stimulatory and suppressive cytokines IL-2 and TGF-β. TGF-β suppresses the immune system by inhibiting the activation of effector cells and reducing tumor antigen expression. It also stimulates tumor growth by promoting angiogenesis, explaining the inclusion of an angiogenic switch mechanism for TGF-β activity. The model predicts that increasing the rate of TGF-β production for reasonable values of tumor antigenicity enhances tumor growth and its ability to escape host detection. The model is then extended to include siRNA treatment which suppresses TGF-β production by targeting the mRNA that codes for TGF-β, thereby reducing the presence and effect of TGF-β in tumor cells. Comparison of tumor response to multiple injections of siRNA with behavior of untreated tumors demonstrates the effectiveness of this proposed treatment strategy. A second administration method, continuous infusion, is included to contrast the ideal outcome of siRNA treatment. The model's results predict conditions under which siRNA treatment can be successful in returning an aggressive, TGF-β producing tumor to its passive, non-immune evading state.

1. **Introduction.** While the struggle to find an effective and permanent cure for cancer continues to challenge scientists, much progress has been made in discovering new information and successful treatments to reduce and even clear tumors. Of fundamental importance is the immune system's apparent failure to combat many types of cancers. Tumors are derived from one or more normal cells that have undergone malignant transformation. The immune response to tumors depends on how antigenic the tumor is. A cell that has undergone significant mutation results in a tumor that is easier to recognize as foreign (i.e. more antigenic) than one that

1991 *Mathematics Subject Classification.* 37C45.
Key words and phrases. mathematical model, tumor, immune response, siRNA.

differs only slightly from a healthy cell. The adaptive immune response relies on four main effector cells to eliminate or slow tumor growth: two types of T cells, phagocytic cells, and killer cells. CD4+ T cells, when stimulated through antigen presentation by macrophages or dendritic cells, secrete the cytokine interleukin-2 (IL-2) to stimulate proliferation of T cells. Activated CD8+ T cells differentiate into cytotoxic T cells (CTLs) and can directly kill tumor cells. Phagocytic cells and natural killer cells identify and destroy tumor cells by recognizing different targets on the tumor cells than do CTLs, thus widening the scope of tumor cell killing. The strength of the immune response greatly impacts success or failure of the immune system's attack on tumor cells. These dynamics we describe comprise a positive feedback loop. Other protein modifiers are responsible for down-regulating the system (such as TGF-β, IL-10, and PGE-2). In analyzing the immune system's inability to clear tumors, it is essential to determine ways that tumor cells are able to evade immune surveillance and methods to potentially boost tumor immunity.

1.1. **Previous Investigations of Tumor-Immune Dynamics.** Previous mathematical modeling efforts have helped to shape our understanding of tumor-immune dynamics (for a review see [1]). What has recently become of great interest in cancer research is the role of pro- and anti-inflammatory molecules, known as cytokines, that participate in orchestrating the immune response as outlined above. Exogenous treatment with these cytokines or with cells that have been activated and re-injected at the site of infection (known as adaptive immunotherapy with tumor-infiltrating lymphocytes (TIL)) has shown conflicting results [5]. To this end, [13] presented the first mathematical model exploring the role of IL-2, a cytokine that enhances T cell growth, on tumor-immune dynamics. Their results indicated that there was no situation in which the tumor could be cleared by the body, except when indefinite treatment with both types of therapy simultaneously was considered. During treatment with these immune boosters (known generally as immunotherapy) IL-2 alone did lead to tumor clearance, but at the expense of immune over-stimulation [13]. In an attempt to combat this destructive result while still maintaining the benefit of tumor clearance, we explore the role of an anti-inflammatory cytokine that counters immune over-stimulation. An interesting aspect of anti-inflammation is that tumor cells have developed mechanisms to harness immunosuppressive machinery to their advantage.

1.2. **The Role of Anti-Inflammatory Cytokines in Tumor Growth.** While the immune system uses both pro- and anti-inflammatory cytokines in response to pathogens in effective ways, tumor cells have developed ways to either circumvent their effects or directly inhibit (or enhance) them. Tumors can evade immune surveillance by secreting immuno-suppressive factors such as interleukin-10 (IL-10), prostaglandin E2 (PGE-2), and transforming growth factor-beta (TGF-β) [25].

While the inhibitory elements included in the model could represent any of these three inhibitory molecules, we will focus on TGF-β because of its extensively studied suppressive and angiogenic properties. By countering the immuno-stimulatory properties of IL-2 and cloaking the tumor from immune system identification, TGF-β inhibits activation and expansion of CTLs and B cells and reduces antigen expression, thereby preventing tumor destruction [25].

TGF-β, which is present in both healthy and tumor cells, plays a beneficial role in normal wound healing, inflammation, and growth stimulatory angiogenesis (new blood vessel formation) [6, 18]. Although this promotes healthy cell growth and function, the production of TGF-β by tumor cells greatly challenges the immune

system through the promotion of angiogenesis, enhancing tumor growth and metastasis [6]. TGF-β is not produced consistently among all tumor cells. Experiments have shown that small tumors (which receive ample nutrient from surrounding tissue) produce little or no TGF-β [20]. Most large tumors, however, do secrete TGF-β and rely heavily on its growth stimulatory effects as well as immuno-suppressive properties [20]. This difference helped to identify the concept that tumors can 'switch' to express immuno-suppressive properties (i.e. produce TGF-β) at a certain stage by accumulating genetic alterations that modify gene expression [20].

To combat immune suppression by tumor cells, we also consider a novel treatment strategy known as small interfering RNA (siRNA) therapy. Uncovering the interplay of stimulatory and inhibitory elements at work during the immune response to tumors can aid in developing better treatment strategies.

1.3. **Immunotherapy of tumors with cytokines and siRNA.** Treatment of solid, malignant tumors occurs in three main ways: traditional chemotherapy, radiation therapy, and immunotherapy. The goal of the latter is to boost (or suppress) the appropriate immune response to assist the body in combating the tumor, rather than affect the tumor directly. Some of the first immuno-therapeutic approaches to attack tumors focused on adoptive transfer of non-specifically *ex vivo*-stimulated host lymphocytes (such as lymphocyte activated killer cells (LAK) and TIL immunotherapy). The amount of TGF-β production by tumors correlates with the stage of disease and the tumor load, explaining why tumors treated in many immunotherapeutic studies may produce enough TGF-β to inhibit activity of LAK or TIL cells [6]. Thus, new approaches using combination therapies must be implemented.

siRNA treatment involves initial delivery of double-stranded RNA (dsRNA) into tumor cells (see Figure 1). The enzyme Dicer then cuts the dsRNA into 21-23 nucleotide-long segments known as siRNAs that, once bound to the RNA-induced silencing complex (RISC), target TGF-β mRNA [15]. The antisense sequence of the siRNA detects complementary mRNA strands that code for TGF-β within tumor cells and the RISC binds to and cleaves the mRNA to prevent TGF-β protein from being produced. Although not yet tested *in vivo*, siRNA treatment should provide a reasonable means of blocking the creation of TGF-β gene product. Ultimately, siRNA treatment works to inhibit TGF-β expression by targeting the specific mRNA sequence which leads to its synthesis, providing a possible solution to the multiple functions of TGF-β that negatively regulate cell proliferation and lead to large tumor mass. Nevertheless, some drawbacks exist that may limit the effectiveness of this therapeutic strategy, including the accessibility of siRNA target sites on TGF-β mRNA [11]. Ideally, cytokine therapy (e.g. IL-2 therapy) can be administered in combination with neutralization strategies, such as siRNA, to inhibit the production and immuno-suppressive effects of TGF-β [6].

Further research and experimentation with these combination therapies may provide an effective solution in addressing the immuno-suppressive effects of TGF-β.

2. **Aggressive Tumor Model.** To model the events described above, we build on the previously published model [13] that describes temporal changes in effector cells, $E(t)$; tumor cells, $T(t)$; and IL-2, $I(t)$. In this paper, we incorporate TGF-β's immuno-suppressive and growth stimulatory effects by defining a new variable, $S(t)$. A model for the dynamics of these cells and cytokines is given below:

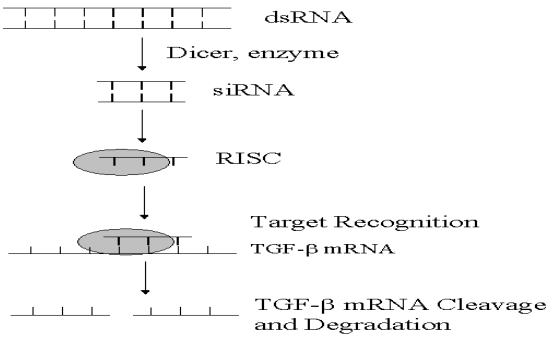

FIGURE 1. A model for the sequence of molecular events associated with siRNA silencing of TGF-β RNA.

$$\frac{dE}{dt} = \frac{cT}{1+\gamma S} - \mu_1 E + \left(\frac{EI}{g_1 + I}\right)\left(p_1 - \frac{q_1 S}{q_2 + S}\right), \tag{1}$$

$$\frac{dT}{dt} = rT\left(1 - \frac{T}{K}\right) - \frac{aET}{g_2 + T} + \frac{p_2 ST}{g_3 + S}, \tag{2}$$

$$\frac{dI}{dt} = \frac{p_3 ET}{(g_4 + T)(1 + \alpha S)} - \mu_2 I, \tag{3}$$

$$\frac{dS}{dt} = \frac{p_4 T^2}{\tau_c^2 + T^2} - \mu_3 S, \tag{4}$$

with initial conditions

$$E(0) = E_0 \qquad T(0) = T_0 \qquad I(0) = I_0 \qquad S(0) = S_0. \tag{5}$$

In equation (1), effector cells are assumed to be recruited to the tumor site as a direct result of the presence of tumor cells. The parameter c in the first term of (1), representing the *antigenicity* of the tumor, measures the ability of the immune system to recognize tumor cells. Antigenicity was shown to be the main bifurcation parameter in [13] governing equilibrium dynamics. The production of TGF-β has been shown to reduce antigen expression, thereby limiting the level of recruitment, measured by inhibitory parameter γ [6]. The second term represents loss of effector cells due to cell death, and the third term, a proliferation term, asserts effector cell proliferation is dependent upon the presence of the cytokine IL-2 and is decreased when the cytokine TGF-β is present. The Michaelis-Menten forms of components of the proliferation term can be derived by considering the binding of IL-2 and TGF-β to effector cell surface receptors, invoking the law of mass action, and making use of usual quasi-steady state assumptions. Therefore, p_1 is the maximum rate of effector cell proliferation in the absence of TGF-β, g_1 and q_2 are half-saturation constants, and q_1 is the maximum rate of anti-proliferative effect of TGF-β.

Equation (2) describes the growth of the tumor population, and the first term represents logistic growth dynamics with intrinsic growth rate r and carrying capacity K in the absence of effector cells and TGF-β (other growth terms were studied in [13] and no significant difference in the dynamics were noted). The second term models the reduction of the tumor population due to immune clearance. This

term was derived so that the net rate of immune-induced tumor cell death $\frac{aE}{g_2+T}$ increases as the effector cell population increases, but decreases as the tumor population increases. The parameter a measures the strength of the immune response to tumor cells and, as expected, was shown to be a bifurcation parameter in [13]. The third term in (2) accounts for the increased growth of tumor cells in the presence of TGF-β. TGF-β is known to stimulate tumor growth by promoting angiogenesis and increasing the intra-tumoral blood supply [18]. Thus, in the presence of TGF-β, tumor size may exceed its carrying capacity. Michaelis-Menten kinetics, where p_2 is the maximum rate of increased proliferation and g_3 is the half-saturation constant, indicate a limited response of tumor cells to this growth-stimulatory cytokine.

The kinetics of IL-2 are described in equation (3). The first term represents IL-2 production which is produced at a maximal rate of p_3 in the presence of effector cells stimulated by their interaction with the tumor cells. In the absence of TGF-β, this a self-limiting process with half-saturation constant, g_4. The presence of TGF-β inhibits IL-2 production in an uncompetitive manner, where the parameter α is a measure of inhibition [17]. Finally, μ_2 represents the decay rate of IL-2.

The fourth equation describes the rate of change of the suppressor cytokine, TGF-β. Experimental evidence suggests that TGF-β is produced in very small amounts when tumors are small enough to receive ample nutrient from the surrounding tissue. However, as the tumor population grows sufficiently large, tumor cells suffer from the lack of oxygen and begin to produce TGF-β in order to stimulate angiogenesis and to evade the immune response once tumor growth resumes [20, 6]. This switch in TGF-β production is modeled by the first term in (4). Here, p_4 is the maximum rate of TGF-β production and τ_c is the critical tumor cell population at which the switch occurs. The decay rate of TGF-β is represented by μ_3.

2.1. **Parameter Estimation.** There are several parameters which mediate the tumor-host interactions described by equations (1-4). Where possible, these parameters are taken from the current medical literature, and for those parameters which no experimental data is available, the goal is to quantify their influence on the model behavior. Table 1 lists the baseline values of the model parameters used in the numerical simulations and their source where appropriate. Briefly, values for the parameters where $S(t) \equiv 0$ presented in [13] are used directly. The parameter p_2 assumes that the presence of TGF-β can increase the net proliferation rate of the tumor cells by at most 50% and, as no data is available, the value of g_3 was initially taken to be the same as g_1. The range of p_4 listed in Table 1 was taken from experiments presented in [23] where levels of TGF-β secretion by γ-ray irradiated and non-irradiated wild-type MBT-2 tumor cells were measured. The values for the parameters q_1 and q_2, representing the immuno-suppressive effects of TGF-β, were estimated from experiments presented in [12] where proliferative inhibition of murine T leukemia cells by cell-secreted TGF-β was measured. In [17], TGF-β regulation of IL-2 expression is investigated and the value of α is estimated from their experiments on the effects of TGF-β on IL-2 secretion by splenocytes and thymocytes. Finally, τ_c is based on the angiogenic switch occurring when 10^6 cells are present, which is based on the experimental observations of [10] showing that tumors can only grow to the nutrient-limited size of approximately 1-2 mm in diameter (and contain $O(10^6)$ cells) without the initiation of their own blood supply.

TABLE 1. *List of baseline parameter values used in simulations and their sources.*

Parameter	Value	Reference
μ_1	$0.03\ days^{-1}$	[14, 7][a]
p_1	$0.1245\ days^{-1}$	[14]
g_1	$2 \times 10^7\ \frac{pg}{l}$	[13]
c	$0 - 0.035\ days^{-1}$	[13]
q_1	$0.1121\ days^{-1}$	[12]
q_2	$2 \times 10^6\ \frac{pg}{l}$	[12]
r	$0.18\ days^{-1}$	[13]
K	$1 \times 10^9\ \frac{cells}{ml}$	[7]
a	$1\ day^{-1}$	[13]
g_2	$1 \times 10^5\ \frac{cells}{ml}$	[13]
p_2	$0.27\ \ days^{-1}$	
g_3	$2 \times 10^7\ \frac{pg}{ml}$	
p_3	$5\ \frac{pg}{cell \times days}$	[13][b]
g_4	$1 \times 10^3\ \frac{cells}{ml}$	[13]
μ_2	$10\ days^{-1}$	[13]
α	$1 \times 10^{-3}\ \frac{l}{pg}$	[17]
μ_3	$10\ days^{-1}$	
τ_c	$1 \times 10^6\ \frac{cells}{ml}$	[10]
p_4	$0 - 3 \times 10^8\ \frac{pg}{l \times days}$	[23]

[a] Average of the values estimated by [14, 7]
[b] This value given in [13] has units of $1/time$; our value is obtained assuming IL-2 saturation at $\approx 2 \times 10^8\ pg/l$ and average cell density of $2 \times 10^8\ cells/l$.

2.2. **Nondimensionalization.** The model presented is a stiff system of differential equations and an appropriate non-dimensional scaling is essential for numerical accuracy. The equations are nondimensionalized as follows:

$$\begin{aligned} w &= \frac{E}{g_2} \quad x = \frac{T}{g_2} \quad y = \frac{I}{g_1} \quad z = \frac{S}{g_3} \quad \bar{t} = \mu_2 t, \\ \bar{\mu}_i &= \frac{\mu_i}{\mu_2} \quad \bar{c} = \frac{c}{\mu_2} \quad \bar{\gamma} = \gamma g_3 \quad \bar{p}_1 = \frac{p_1}{\mu_2} \quad \bar{p}_2 = \frac{p_2}{\mu_2}, \\ \bar{p}_3 &= \frac{p_3 g_2}{\mu_2 g_1} \quad \bar{q}_1 = \frac{q_1}{\mu_2} \quad \bar{q}_2 = \frac{q_2}{g_3} \quad \bar{r} = \frac{r}{\mu_2} \quad \bar{K} = \frac{K}{g_2}, \\ \bar{a} &= \frac{a}{\mu_2} \quad \bar{g}_4 = \frac{g_4}{g_2} \quad \bar{\alpha} = \alpha g_3 \quad \bar{p}_4 = \frac{p_4}{\mu_2 g_3} \quad \bar{\tau}_c = \frac{\tau_c}{g_2}. \end{aligned} \tag{6}$$

After dropping the over-bar notation for convenience, the system describing tumor evasion of immune surveillance in the absence of treatment may be written as follows

$$\frac{dw}{dt} = \frac{cx}{1+\gamma z} - \mu_1 w + \left(\frac{wy}{1+y}\right)\left(p_1 - \frac{q_1 z}{q_2+z}\right), \tag{7}$$

$$\frac{dx}{dt} = rx\left(1-\frac{x}{K}\right) - \frac{awx}{1+x} + \frac{p_2 xz}{1+z}, \tag{8}$$

$$\frac{dy}{dt} = \frac{p_3 wx}{(g_4+x)(1+\alpha z)} - y, \tag{9}$$

$$\frac{dz}{dt} = \frac{p_4 x^2}{\tau_c^2 + x^2} - z, \tag{10}$$

with initial conditions

$$w(0) = w_0 \qquad x(0) = x_0 \qquad y(0) = y_0 \qquad z(0) = z_0. \tag{11}$$

3. **Pre-treatment Tumor Growth.** Due to the highly nonlinear nature of this system, we restrict our attention to numerical analysis of the model equations in order to characterize the dynamic behavior and quantify the influence of the parameter values. A steady state analysis of (7) - (10) with $S(t) = 0$ is presented in [13].

3.1. **Passive Tumors (i.e. No TGF-β Production).** In this section, passive tumors are defined as those which do not actively produce TGF-β in order to enhance its growth and to evade immune detection. Numerical analysis of the model equations in absence of the immuno-suppressive and growth stimulating abilities of tumor cells ($S(t) = 0$) is reported in [13]. As this previous investigation is the starting point for our new model, a brief summary of the results is given below. All parameters, as well as the variable time, mentioned in the text henceforth are nondimensional unless otherwise noted.

Table 2 shows how the number and stability of the tumor cell steady states vary with antigenicity of the tumor, c, highlighting three regions of interest. In the first range of values ($0 < c < 8.55 \times 10^{-6}$) the single stable steady state corresponds to a large tumor mass growing very near to its carrying capacity. Therefore, the tumor has successfully evaded immune recognition by expressing antigens which are difficult to detect as foreign.

In the second range, ($8.55\times10^{-6} < c < 0.0032$), a stable limit cycle indicates that the tumor spends a portion of time near its carrying capacity and then lies dormant (mass near zero) for another period of time. As c increases, the magnitude and period of oscillations decrease, resulting in smaller tumor size and quicker recovery time. The last range of values ($0.0032 < c$) begins at a Hopf bifurcation followed by the emergence of a stable, spiral node. The damped oscillations produced here lead to a small persistent tumor that, although is never entirely cleared, can be described as dormant. During times when the tumor cell population is oscillating with a peak of nearly ninety percent of its carrying capacity, it is very possible that the host will not survive this stage long enough for the tumor to reach a period of dormancy. Hence, we cannot assume the host will be able to wait for the immune system to elicit a period of dormancy. In addition, while this analysis shows the possible outcomes for a passive tumor can be favorable if c is sufficiently large, it must also be recognized that the outcome can be significantly less promising if the tumor were aggressive and began producing TGF-β to enhance its growth and evade immune surveillance.

TABLE 2. *Summary of the predicted behaviors of passive and aggressive tumors.*

Antigenicity, c	Stability[a]	Tumor Behavior
	Passive Tumors	
	(Equations 1-5, $S(t) \equiv 0$)	
$0 < c < 8.55 \times 10^{-6}$	Asymptotically stable node	Large Tumor Mass
$8.55 \times 10^{-6} < c < 0.0032$	Hopf bifurcation to stable limit cycles	Tumor mass oscillates between dangerously high and encouragingly low values with amplitude and period decreasing with increasing c.
$0.0032 \leq c$	Hopf bifurcation to stable, spiral node.	Damped oscillations to small, dormant tumor mass
	Aggressive Tumors[b]	
	(Equations 1-5, $S(t) \neq 0$)	
$0 < c < 8.55 \times 10^{-6}$ (Figure 2)	Asymptotically stable node	Large Tumor Mass
$8.55 \times 10^{-6} < c < 0.0032$ (Figure 3)	As tumor becomes more aggressive, that is as p_4 increases, limit cycles give way to stable node via Hopf bifurcation	For small p_4, tumor oscillates between dangerously high and encouragingly low values with amplitude and period decreasing with increasing c. As p_4 increases, a large tumor mass results.
$0.0032 \leq c$ (Figure 4)	As tumor becomes more aggressive, a stable, spiral node gives way to a stable node	For small p_4, tumor is small and dormant; as p_4 increases, a large tumor mass results.

[a] Stability refers to that of the tumor-present steady states.
[b] Aggressive behavior is measured by the parameter, p_4. A large p_4 value indicates that the tumor is vigorously producing TGF-β in order to promote its own growth and to suppress the immune response.

3.2. **Aggressive Tumor (i.e. TGF-β Production).** We next examine the case in which tumors are aggressive interferers of the body's immune response. To do so, we consider the effect on the model when TGF-β is introduced, causing increased tumor growth from angiogenesis and the increased ability of the tumor to escape detection by the immune system due to immuno-suppressive properties. Although the addition of TGF-β to the model indicates qualitatively parallel behavior with the original model in [13], several important quantitative differences also occur. For example, a large tumor mass growing near its carrying capacity will ultimately occur for all tumors at some p_4 value, regardless of the level of antigenicity. This behavior is substantially different from that of passive tumors, which only experience uncontrolled tumor growth for values of c below 8.55×10^{-6}. This shows the obvious outcome that aggressive tumors are even more destructive to the host than passive tumors and will likely be harder to control. The following three figures depict the different results when increasing the maximum rate of TGF-β production (p_4) for various values of antigenicity (c), and antigenic inhibition (γ). Upon varying these parameter values, we expect to see very different outcomes for control of the tumor (for a summary, see Table 2).

In Figure 2, the value of c is very small (5×10^{-6}), preventing tumor detection by the host immune system. This results in rapid tumor growth (even in the absence of TGF-β, see Table 2) which quickly approaches the environmental carrying capacity. For all values of p_4 greater than zero, tumor growth even surpasses the normal carrying capacity that exists in the absence of TGF-β. All values of γ yield uncontrolled growth in this case.

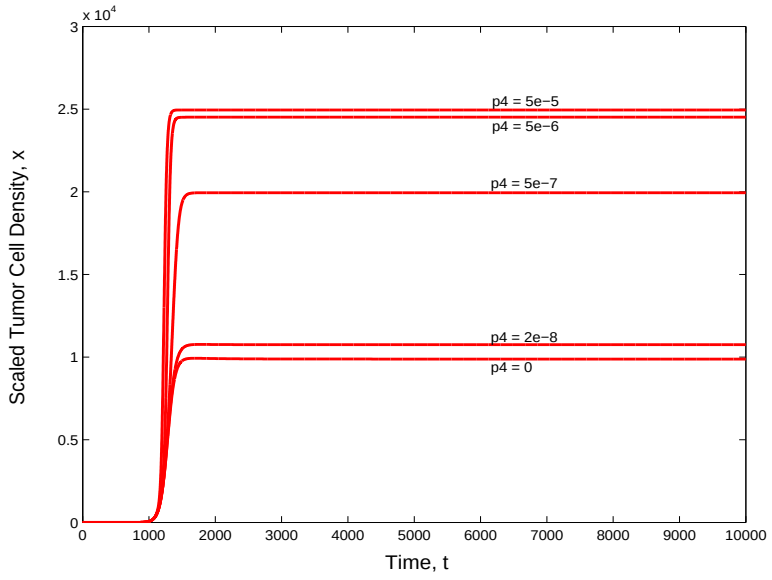

FIGURE 2. A numerical simulation of the model equations (7-11) plotting the scaled tumor cell density versus time for a hard to detect tumor ($c = 5^{-6}$) as the rate of TGF-β production, p_4, increases.

Figure 3 ($c = 0.002$) shows an intermediate value of c at which uncontrolled tumor growth is suppressed. Instead, there is a critical change in tumor behavior

once the value of p_4 increases to a Hopf bifurcation ($p_4 = 0.12$) (Figure 3a). The tumor-present steady state is unstable for small values of p_4, resulting in a limit cycle, characterized by oscillations that depict periods of time spent near carrying capacity followed by periods of dormancy. After reaching the Hopf bifurcation, a stable steady state emerges representing a large tumor mass (Figure 3d). Note that for some values of p_4 there are three possible steady states. The behavior that characterizes the stable steady state will predominate in these cases. In Figure 3, we used $\gamma = 10$. Decreasing γ requires a higher level of TGF-β production (p_4) to result in the same behavior. Section 3.2.1 examines this relationship more closely.

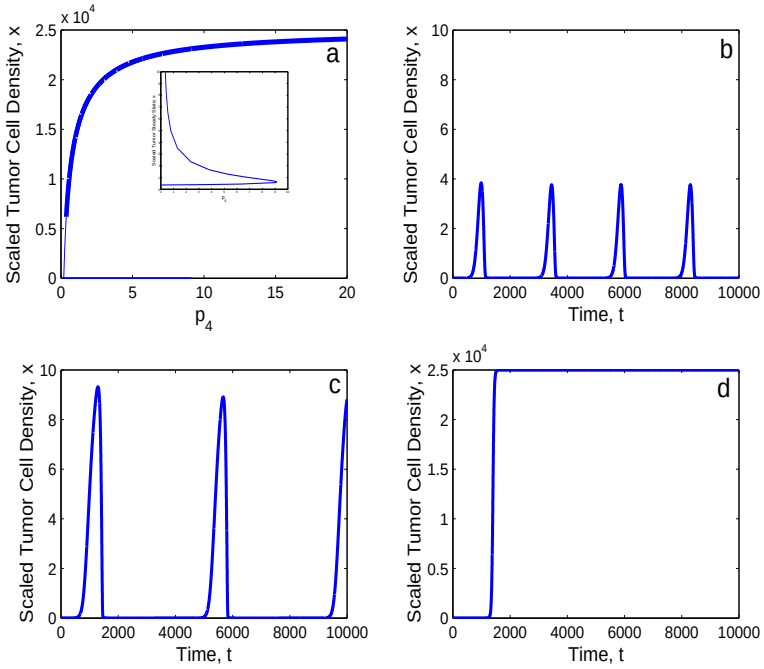

FIGURE 3. (a) Bifurcation diagram showing changes in the number and stability of the steady states associated with the scaled tumor cell density (x) as the rate of TGF-β production varies. A Hopf bifurcation occurs when $p_4 = 0.1205$. The thin line represents unstable behavior and the thick line corresponds to stable tumor behavior for antigenicity value $c = 0.002$. The inset highlights the region of instability near $p_4 = 0$. The remaining graphs are numerical simulations of the model equations (7-11), giving the scaled tumor cell density per time as p_4 increases to the following values: (b) $p_4 = 0$ (c) $p_4 = 0.1204$ (d) All $p_4 > 0.1204$.

Finally, Figure 4 ($c = 0.0035$) represents the lowest value of c at which the immune system can initially control the tumor. The behavior is characterized by damped oscillations that reduce to a low steady state, and the tumor can be described as dormant. However, as p_4 increases past the Hopf bifurcation ($p_4 = 2.85$, Figure 4a), the immune system is no longer successful in defeating the tumor, and large tumor mass again characterizes the tumor behavior near carrying capacity (Figure 4d).

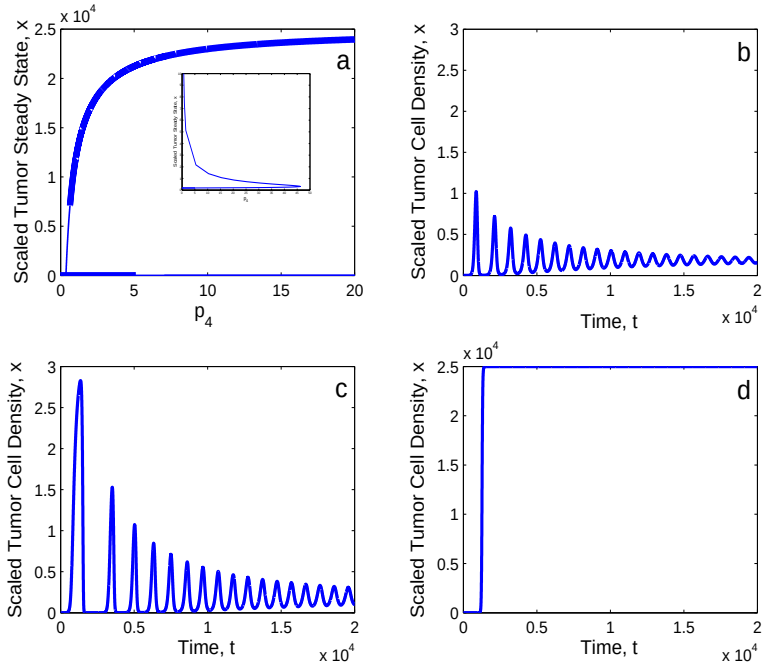

FIGURE 4. (a) Bifurcation diagram characterized by one Hopf bifurcation at $p_4 = 2.84$. The thin line represents unstable behavior and the thick line corresponds to stable tumor behavior for antigenicity value $c = 0.0035$. The inset highlights the changes in stability near $p_4 = 0$. The remaining graphs are numerical simulations of the model equations (7-11), giving the tumor cell density per time as p_4 increases to the following values: (b) $p_4 = 0$ (c) $p_4 = 2.84$ (d) All $p_4 > 2.84$.

3.2.1. *Role of Antigen Expression.* Figure 5 shows the interplay between γ and the p_4 values at which the Hopf bifurcation occurs (here $c = 0.0035$). Recall that γ is the measure of the ability of TGF-β to reduce antigen expression, c. As this level of inhibition increases, the magnitude of p_4 at which the Hopf bifurcation occurs decreases. In other words, the greater the ability of TGF-β to reduce antigen expression, the lower the rate of production of TGF-β is needed to overtake the immune system. This two parameter bifurcation diagram therefore illustrates the important trade-off between host recognition and tumor evasion in aggressive tumors.

In summary, because aggressive tumors inhibit IL-2 production, reduce antigen expression, and promote tumor growth, no values of c between 5×10^{-6} and 0.0032 are able to permanently give way to the dormancy that was reached for passive tumors. Such a result suggests that the roles of c, p_4, and γ are significant.

3.2.2. *Role of Immune Efficacy.* Recalling that parameter a, the measure of the strength of the immune response, greatly impacts the behavior of the model, we now analyze the effect of varying the value of a in the aggressive tumor case (without treatment). Figure 6 includes curves that show the values of a for which there is a change in stability from uncontrolled tumor behavior to periodic or damped

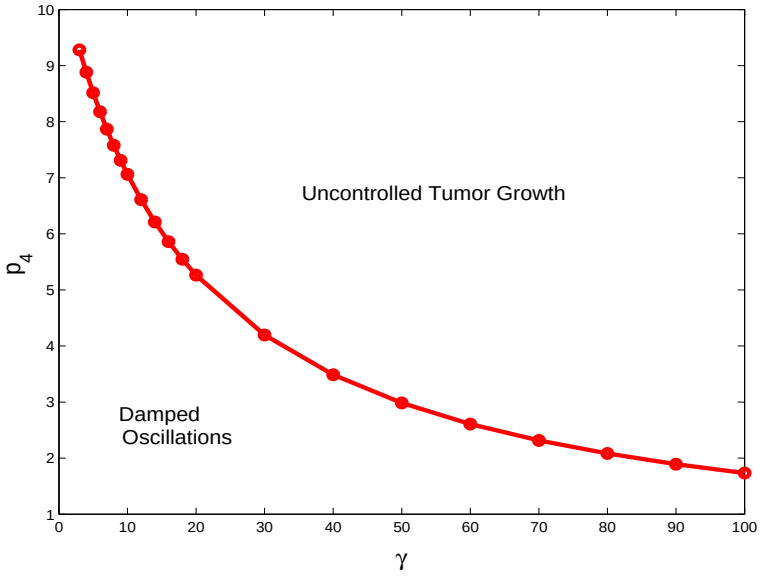

FIGURE 5. Two-parameter bifurcation diagram which relates host recognition (γ) and tumor evasion (p_4) for $c = 0.0035$, representing the most recognizable tumors. In this figure, the $p_4 - \gamma$ parameter space is separated into regions of controlled and uncontrolled tumor growth. For values of these parameters below the curve, tumor behavior is characterized by damped oscillations to a small steady state representing a dormant tumor mass. Above the curve, the tumor will grow uncontrollably.

oscillations. These values of a are plotted against increasing antigenicity values (c) in order to illustrate the relationship between these two parameters. As the antigenicity increases, the strength of the immune response required to achieve oscillatory behavior decreases. This follows since the immune response is more successful against tumors characterized by a high level of antigen expression. The three different curves depict the behavior for increasing rates of TGF-β production. As the curves confirm, more aggressive tumors require a stronger immune response than do less aggressive tumors. It is important to note that while it is mathematically possible to find a value of a for which tumor growth is oscillatory despite the level of antigenicity, values of a greater than 0.2 are not biologically sensible. Later, when we compare these results to those we obtain with treatment, we will be able to conclude that there exists a realistic level of immune response (in the range $a = 0.1$ to 0.3) with corresponding critical values of c for which the body can partially control the tumor for various levels of TGF-β production. Notice from Figure 6 that these include $c \geq 0.001$ for $p_4 = 5 \times 10^{-5}$, $c \geq 0.0015$ for $p_4 = 0.005$, and $c \geq 0.002$ for $p_4 = 0.5$.

4. **siRNA Treatment Model.** In this section, we explore an alternate immunotherapeutic approach that utilizes siRNA strands to suppress TGF-β production and thereby restore the success of traditional immunotherapy. Thus, we extend our math model to include siRNA treatment, which directly blocks TGF-β expression

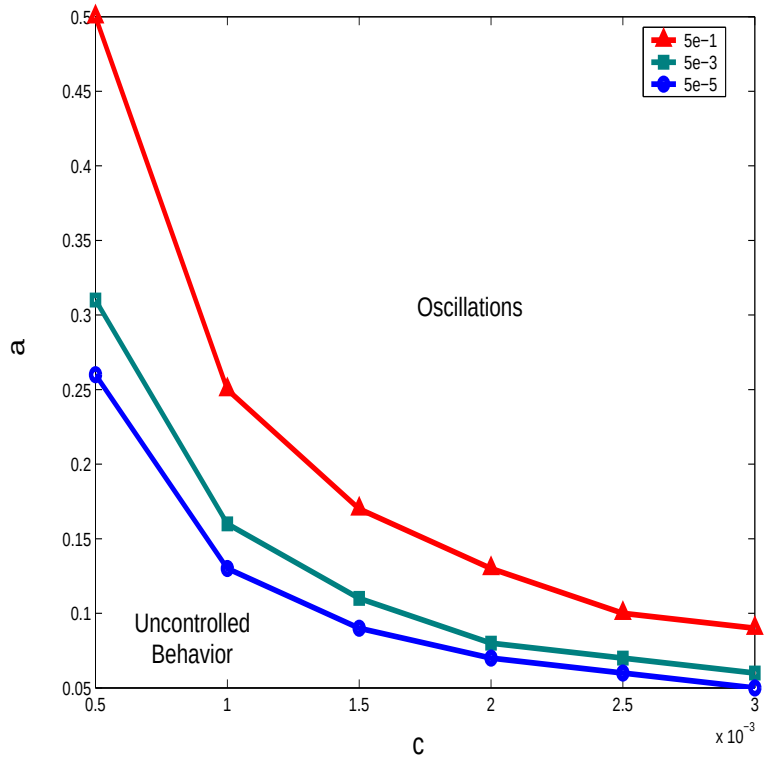

FIGURE 6. Two-parameter bifurcation diagram which reveals the interplay between the strength of the immune response (a) and tumor antigenicity (c). In this figure, the $a-c$ parameter space is separated into regions of controlled and uncontrolled tumor growth. Three curves are shown, each with an increasing value of TGF-β production (p_4). For parameter values below each curve, respectively, the tumor will grow uncontrollably. Above the curve, the tumor oscillates to a small stable steady state. Note the range $a = 0.1$ to $a = 0.13$ gives realistic levels for the strength of the immune response.

in tumor cells, rendering the once aggressive cells passive. In accordance with the above description of siRNA treatment, the model equations (1-4) are modified as follows in order to incorporate the effects that the siRNA treatment will have on tumor cells and TGF-β expression.

$$\frac{dE}{dt} = \frac{cT}{1+\gamma S} - \mu_1 E + \left(\frac{EI}{g_1+I}\right)\left(p_1 - \frac{q_1 S}{q_2+S}\right), \tag{12}$$

$$\frac{dT}{dt} = rT\left(1-\frac{T}{K}\right) - \frac{aET}{g_2+T} + \frac{p_2 ST}{g_3+S}, \tag{13}$$

$$\frac{dI}{dt} = \frac{p_3 ET}{(g_4+T)(1+\alpha S)} - \mu_2 I, \tag{14}$$

$$\frac{dS}{dt} = \frac{p_4 T^2}{\tau_c^2 + \left(1+\frac{fA}{k_i}\right)T^2} - \mu_3 S, \tag{15}$$

$$\frac{dA}{dt} = D_i(t) - \mu_4 A, \qquad i = 1 \text{ or } 2 \tag{16}$$

Notice that equations (12), (13), and (14) are identical to equations (1), (2), and (3), respectively. Equation (15) is the modified version of equation (4) that describes the rate of change of the extracellular concentrations of the cytokine, TGF-β. The first term in equation (15) assumes that the production of extracellular TGF-β is inhibited as a result of the siRNA that is bound to the target TGF-β mRNA. Variable A represents total free and bound strands of siRNA, with parameter f as the proportion of A that is bound. Thus, fA represents the bound siRNA strands. The siRNA acts as an uncompetitive inhibitor of the suppressor with inhibition rate constant k_i. While this term still accounts for the switching mechanism that characterizes the size of cell that produces TGF-β, the new feature is the description of how siRNA treatment suppresses the production of TGF-β. Equation (16) describes the injection and degradation of the siRNAs. The first term, $D_i(t)$, represents the dose of free (unbound) siRNAs as a function of time, where $i = 1, 2$ and D_1 describes a continuous infusion dose and D_2 describes a multiple injection dose, and both are defined here:

$$\begin{aligned} D_1(t) &= D_0 \ \equiv \ \text{constant} \\ D_2(t) &= D_0 \ \Sigma_{i=1}^{n} \ e^{-(t_i - t)^2/\epsilon} \end{aligned} \tag{17}$$

Note that D_0 is the injected dose, the t_i's are the specific times of injection, n is the number of injections (here we will use n = 11), and $\epsilon = 10$. The parameter μ_4 in the second term of equation (16) represents the decay of the free siRNA strands based on their half life. In deriving this final equation, we first examined the rates of change for the free and bound siRNA separately. Consider the following two equations:

$$\frac{dA_{free}}{dt} = D_i(t) - \mu_4 A_{free} - k_a A_{free}\left([RS] - A_{bound}\right) + k_d A_{bound} \tag{18}$$

$$\frac{dA_{bound}}{dt} = k_a A_{free}\left([RS] - A_{bound}\right) - k_d A_{bound} \tag{19}$$

Equation (18) shows that the initial dose of free siRNAs given as a function of time, $D_i(t)$, is decreased by an siRNA death rate (μ_4). The third term describes the binding of the free siRNA to the TGF-β mRNA (denoted [RS]), which occurs at an association rate k_a. Notice A_{bound} is subtracted from [RS] in order to depict the actual concentration of TGF-β mRNA sites still available for binding. The fourth term allows for reversible binding, which occurs at a dissociation rate k_d. This term suggests that proteins can bind but then release. Equation (19) gives the

population of bound siRNA, which is decreased by dissociation. By modeling the decreased production of TGF-β due to free siRNA, we are capturing the concept that bound siRNA effectively eliminates TGF-β mRNA. In order to derive the rate of change equation for the total amount of siRNA present in the system, we sum (18) and (19) deriving equation (16). Note that $A_{free} = (1-f)A$, $A_{bound} = fA$, and $A = A_{free} + A_{bound}$.

4.1. **Nondimensionalization.** Before proceeding to investigate the model numerically, we first recast the equations in nondimensional form. The scaling we use is the same as in (6) with the following additions:

$$\bar{k}_i = \frac{k_i}{fA_0} \quad A_0 = \frac{k_i}{f} \quad \bar{D} = \frac{Df}{\mu_2 k_i} \quad \bar{\mu}_4 = \frac{\mu_4(1-f)}{\mu_2}. \tag{20}$$

After dropping the over-bar notation for convenience, the system describing tumor evasion of immune surveillance in the presence of siRNA treatment may be written as follows:

$$\frac{dw}{dt} = \frac{cx}{1+\gamma z} - \mu_1 w + \left(\frac{wy}{1+y}\right)\left(p_1 - \frac{q_1 z}{q_2+z}\right), \tag{21}$$

$$\frac{dx}{dt} = rx\left(1-\frac{x}{K}\right) - \frac{awx}{1+x} + \frac{p_2 xz}{1+z}, \tag{22}$$

$$\frac{dy}{dt} = \frac{p_3 wx}{(g_4+x)(1+\alpha z)} - y, \tag{23}$$

$$\frac{dz}{dt} = \frac{p_4 x^2}{\tau_c^2 + (1+v)x^2} - z, \tag{24}$$

$$\frac{dv}{dt} = D_i(t) - \mu_4 v, \tag{25}$$

with initial conditions

$$w(0) = w_0, \qquad x(0) = x_0, \qquad y(0) = y_0, \qquad z(0) = z_0, \qquad v(0) = v_0. \tag{26}$$

This model introduces three new parameters: f, μ_4 and D_0. In the presence of free siRNA, the population of TGF-β mRNA will decrease as the siRNA binds to its target. Ninety percent (described by parameter f) of the free siRNA binds to its target TGF-β mRNA [19]. We estimate the decay of this free siRNA (μ_4) to be 0.66 days^{-1} [8]. Also, many *in vitro* studies have evaluated siRNA treatment with an initial dose of 2×10^9 pg/ml of siRNA [24]; therefore, we take $D_0 = 5 \times 10^{10}$ pg/ml as a comparable dose for an *in vivo* system.

4.2. **Numerical Simulations.** When first examining the results of adding siRNA into our system, we consider administering a constant dose of siRNA ($D_1(t)$) to mimic a continuous infusion protocol. Throughout this section we examine the case for an intermediate level of antigenicity ($c = 0.002$) and an aggressive tumor ($p_4 = 0.5, \gamma = 10$). Although this administration is unrealistic in terms of actual treatment techniques, it provides us with a measure of the ideal results when implementing siRNA treatment. When compared to Figure 3 (no treatment), Figure 7 shows that a continuous infusion of siRNA no longer results in uncontrolled tumor growth when $a = 0.12$; instead, the tumor cell density exhibits sustained oscillations with a low amplitude. This result reveals that even the most aggressive form of siRNA treatment cannot completely clear the tumor when the strength of the immune response, a, is at its baseline value. Increasing the strength of the immune

response beyond a critical value ($a = 0.13$) gives treatment results identical to those without treatment. This implies that at such high values of a ($a \geq 0.13$), the body would be capable of controlling the tumor on its own (i.e. without administering treatment); we therefore conclude that acceptable values of a must be less than 0.13.

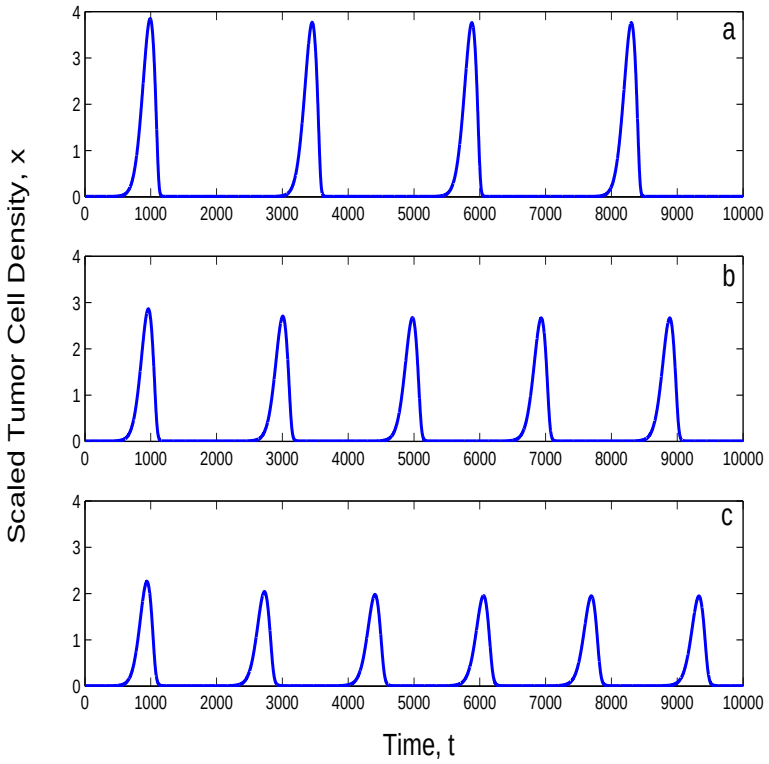

FIGURE 7. Plot of tumor cell density versus time after continuous infusion of siRNA: (a) $a = 0.1$ (b) $a = 0.11$ (c) $a = 0.12$.

Figure 8 incorporates a more realistic administration schedule ($D_2(t)$) consisting of one or more rounds of multiple injections of siRNA. One round of treatment corresponds to siRNA injected once a day for eleven days. As expected, this limited number of injections does not give as favorable an outcome as continuous infusion. For $a = 0.1$ (Figure 8a), tumor behavior begins with a small peak (around $x = 25$), but then becomes uncontrolled at about $t = 5500$, corresponding to the point at which the treatment is no longer having an effect. As values of a increase to 0.1 and 0.12 (Figures 8c and 8e, respectively), the level of the initial peaks decrease, the number of peaks increase, and the time point at which uncontrolled tumor behavior dominates is delayed slightly. Figures 8b, 8d, and 8f show the improved behavior of the system when two rounds of siRNA treatment are administered (at $t = 1000$ and $t = 5500$). An additional round of treatment delays the time at which the tumor becomes uncontrolled. Therefore, this treatment suggests a way to control tumor growth by administering timely injections. Ultimately, siRNA alone cannot lead to damped oscillatory tumor behavior, but can control the tumor with oscillations at a low level.

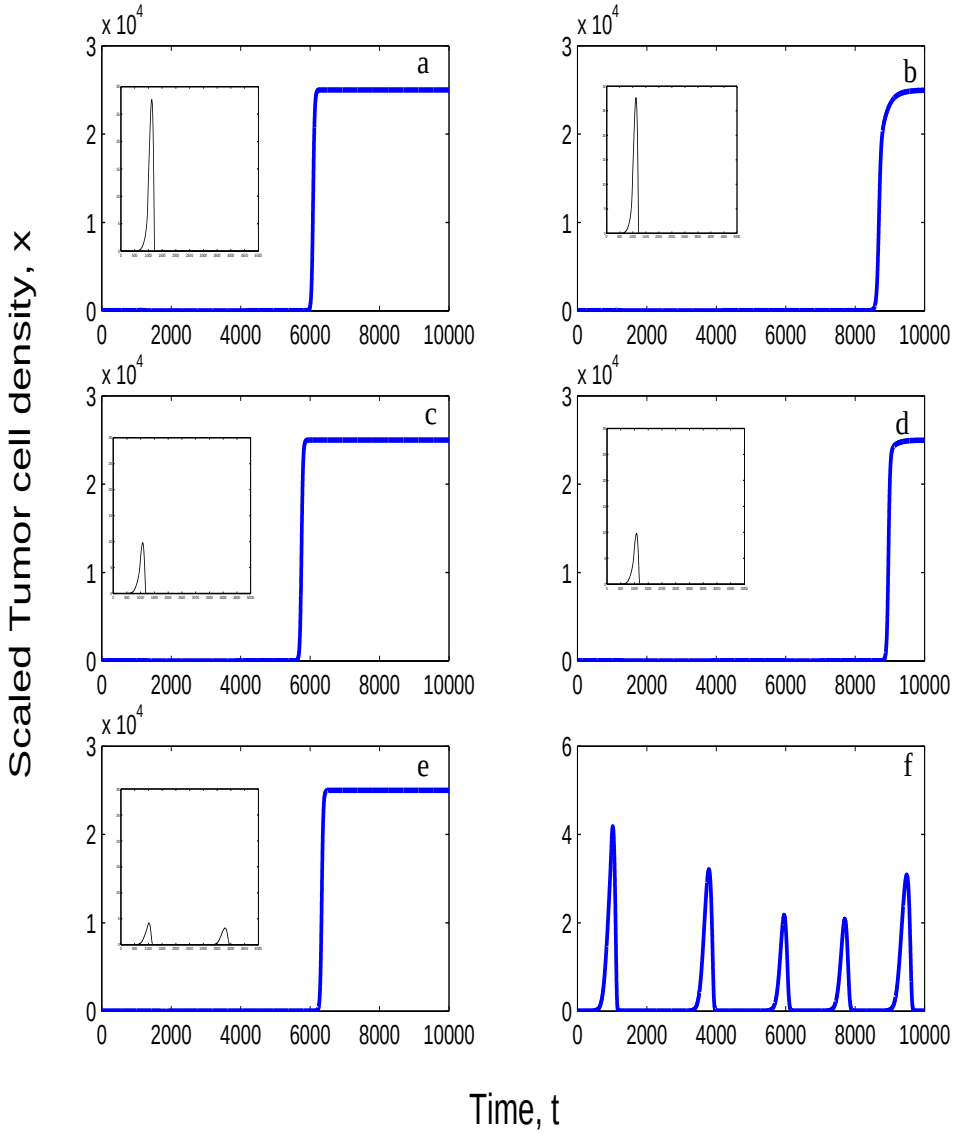

FIGURE 8. Numerical simulations of the siRNA treatment strategy. One round of treatment was administered at time $t = 1000$ in (a), (c), and (e); whereas two rounds of treatment were administered at $t = 1000$ and $t = 5500$ in (b), (d), and (f). Also the immune strength is its baseline value, $a = 0.1$ in (a) and (b) but increases to $a = 0.11$ in (c) and (d) and $a = 0.12$ in (e) and (f). The insets of each figure highlight the region of small oscillations at early times, $t < 5000$.

5. **Discussion.** This paper describes mechanisms by which the cytokines IL-2 and TGF-β mediate the immune response to tumor growth and the added down-regulation of this response by tumor cells. IL-2 plays an important role in orchestrating an immune response to infection by stimulating the activation of effector

cells which target and destroy the invading tumor cells. In contrast, TGF-β inhibits the immune response by suppressing IL-2 production and reducing antigen expression, both of which reduce activation of effector cells. In addition to down-regulating immune cells which combat the tumor, TGF-β also stimulates tumor growth via angiogenesis. Therefore, although TGF-β is beneficial as an anti-inflammatory cytokine in that it helps to prevent the over-stimulation of the immune system, TGF-β also cloaks tumors from immune system detection and aids in their growth. This explains why aggressive tumors which actively produce TGF-β are even more destructive to the host than their passive counterparts.

In order to investigate the potential for growth and immune escape of passive and aggressive tumors, we have developed a mathematical model which describes temporal changes in effector cells, tumor cells, IL-2, and TGF-β. When analyzing the results from passive tumors and aggressive tumors, comparisons of the antigenicity (c) of the tumor and production rate of TGF-β (p_4) are key to explaining significant differences in behavior resulting from the active production of TGF-β by a tumor.

Beginning with values of the tumor antigenicity as small as $c = 0.0001$, a single, unstable steady state exists for passive tumors. In this case, the solutions are characterized by sustained oscillations which correspond to periods of detectable tumor cell concentrations near carrying capacity and longer periods of dormancy. As the value of c increases, the amplitude and period of the limit cycles decrease, causing the magnitude and time spent near the peak to decrease. A Hopf bifurcation marks the end of the sustained oscillations and the emergence of stable steady state for a larger antigenicity, $c = 0.0032$. The approach to steady state is via damped oscillations which eventually results in a persistent tumor that can be defined as dormant.

Unlike the case of passive tumors, uncontrolled tumor growth at or near carrying capacity characterizes the behavior of all aggressive tumors. For intermediate values of antigenicity (e.g. $c = 0.002$), a Hopf Bifurcation exists for which an initial unstable steady state (characterized by sustained oscillations representing periods of tumor activity and dormancy) gives way to a stable steady state (at which uncontrolled tumor growth recurs). Further, unlike passive tumors, tumor dynamics for a very large antigenicity ($c = 0.0032$) do not result in damped oscillations for all values of p_4. Instead, once $p_4 > 2.85$, uncontrolled tumor growth characterizes the behavior of these tumors.

The results from the aggressive tumor analysis are rooted in the dual role of TGF-β. The immune system inhibitory effects (such as blocking IL-2 production and inhibiting antigen-specific T-cell activation) and tumor-stimulating effects (such as increasing blood supply to tumor cells in order to enhance the tumor's ability to metastasize) of TGF-β provide explanation for enhanced tumor growth and failure of the host immune system. In order to counteract this occurrence, the model was extended to include a novel therapeutic strategy using siRNA. siRNA treatment inhibits TGF-β production by binding to the mRNA strands that code for TGF-β, thereby blocking TGF-β synthesis. Thus, the aim of siRNA therapy is to limit the inhibitory effects of TGF-β and remove one potentially deadly immune escape mechanism employed by aggressive tumors. Administering a dose of siRNA daily (for eleven consecutive days) at appropriate time intervals led to controlled oscillatory tumor behavior. While not yielding persistent dormancy, siRNA offers a treatment technique that counteracts the devastating effects of TGF-β, such as IL-2 inhibition and increased tumor growth.

For future study, the addition of IL-2 (e.g. via LAK or TIL treatments) into our treatment model could result in actual tumor clearance, as siRNA would be present to counteract the immuno-suppressive cytokine and IL-2 would be administered to further boost the response of the immune system.

Acknowledgments. D.E.K. would like to thank Dr. J.C. Panetta for helpful discussions in the early development of this model and Ms. Ayla Erguna, Katia Koelle and Erin Cavusgil for early efforts on preliminary model development and simulation. Part of this work was supported under grant awards by the NIH R01HL6119 and R01HL68526 (to DEK) and NSF-DMS #0114473 (to TLJ). J.C.A. gratefully acknowledges financial support provided by the NSF REU program and thanks Mr. Benjamin Singer for his help with XPP/AUTO. All authors thank Dr. David Engelke for helpful information on siRNAs.

REFERENCES

[1] J.A. Adam and N. Bellomo. A survey of models for tumor-immune system dynamics. *Birkhauser, Boston*, 1996.

[2] M.R. Bernsen, J. Tang, L.A. Everse, J.W. Koten, and W. Den Otter. Interleukin 2 (IL-2) therapy: potential advantages of locoregional versus systemic administration. *Cancer Treat. Rev.*, 25:73–82, 1999.

[3] N.J. Caplen, S. Parrish, F. Imani, A. Fire, and R.A. Morgan. Specific inhibition of gene expression by small double-stranded RNAs in invertebrate and vertebrate systems. *Proc. Natl. Acad. Sci.*, 98:9742–9747., 2001.

[4] A. Cerwenka and S.L. Swain. TGF-β1: Immunosuppressant and viability factor for T lymphocytes. *Microbes Infec.*, 1:1291–1296., 1999.

[5] A.E. Chang and S. Shu. Current status of adoptive immunotherapy of cancer. *Crit. Rev. Oncol. Hematol.*, 22:213–228, 1996.

[6] K.E. de Visser and W.M. Kast. Effects of TGF-β on the immune system: Implications for cancer immunotherapy. *Leukemia*, 13:1188–1199, 1999.

[7] R.J. DeBoer, P. Hogeweg, H.F.J Dullens, R.A. De Weger, and W. Den Otter. Macrophage T lymphocyte interactions in the anti-tumor immune response: A mathematical model. *J. Immunol.*, 134:2748–2757, 1985.

[8] S. Elbashir, J. Harborth, W. Lendeckel, A. Yalcin, K. Weber, and T. Tuschl. Duplexes of 21-nucleotide RNAs mediate RNA interference in cultured mammalian cells. *Nature.*, 411:494–498, 2001.

[9] I. Espinoza-Delgado, M.C. Bosco, T. Mussso, K. Mood, F.W. Ruscetti, D.L. Longo, and L. Varesio. Inhibitory cytokine circuits involving transforming growth factor-β, interferon-γ, and interleukin-2 in human monocyte activation. *Blood*, 83:3332–3338., 1994.

[10] J. Folkman and M. Hochberg. Self-regulation of growth in three dimensions. *J. Exp. Med.*, 138:743., 1973.

[11] T. Holen, M. Amarzguioui, M.T. Wiiger, E. Babaie, and H. Prydz. Positional effects of short interfering RNAs targeting the human coagulation trigger tissue factor. *Nucleic Acids Res.*, 30:1757–1766, 2002.

[12] C.l. Hsieh, D.S. Chen, and L.H. Hwang. Tumor-induced immunosuppression: A barrier to immunotherpay of large tumors by cytokine-secreting tumor vaccine. *Hum. Gene Ther.*, 11:681–692, 2000.

[13] D. Kirschner and J.C. Panetta. Modeling immunotherapy of the tumor-immune interaction. *J. Mathem. Biol.*, 37:235–252, 1998.

[14] V.A. Kuznetsov and I.A. Makalkin. Nonlinear dynamics of immunogenic tumors: Parameter estimation and global bifurcation analysis. *Bullet. Mathem. Biol.*, 56:295–321, 1994.

[15] C. Lipardi, Q. Wei, and B.M. Paterson. RNAi as random degradative PCR: siRNA primers convert mRNA into dsRNAs that are degraded to generate new siRNAs. *Cell*, 107:297–307., 2001.

[16] X.W. Mao, J.D. Kettering, and D.S. Gridley. Immunotherapy with low-dose interleukin-2 and anti-transforming growth factor-β antibody in a murine tumor model. *Cancer Biother.*, 9:317–325, 1994.

[17] S.C. McKarns and N.E. Kaminski. TGF-β differentially regulates IL-2 expression and [^{3}H]-thymidine incorporation in CD3ϵ mAb- and CD28 mAb-activated splenocytes and thymocytes. *Immunopharmacology*, 48:101–115, 2000.
[18] M.A. Nash, G. Ferrandina, M. Gordinier, A. Loercher, and R.S. Freedman. The role of cytokines in both the normal and malignant ovary. *Endoc. Rel. Cancer*, 6:93–107., 1999.
[19] A. Nykanen, B. Haley, and P.D. Zamore. ATP requirements and small interfering RNA structure in the RNA interference pathway. *Cell*, 107:309–321., 2001.
[20] F. Paillard. Immunosuppression mediated by tumor cells: A challenge for immunotherapeutic appraoaches. *Hum. Gene Ther.*, 11:657–658, 2000.
[21] G. Storz. An expanding universe of noncoding RNAs. *Science*, 296:1260–1263, 2002.
[22] T. Tuschl. Expanding small RNA interference. *Nature Biotech.*, 20:446–448, 2002.
[23] T.S. Tzai, A.L. Shiau, L.L. Liu, and C.L. Wu. Immunization with TGF-β antisense oligonucleotide-modified autologous tumor vaccine enhances the antitumor immunity of MBT-2 tumor-bearing mice trough upregulation of MHC Class I and Fas expressions. *Anitcancer Res.*, 20:1557–1562, 2000.
[24] F. Wianny and M. Zernicka-Goetz. Specific interference with gene function by double-stranded RNA in early mouse development. *Nature Cell Biol.*, 2:70–75, 2000.
[25] S. Wojtowicz-Praga. Reversal of tumor-induced immunosuppression: A new approach to cancer therapy. *J. Immunol.*, 20:165–177, 1997.
[26] P.D Zamore. Ancient pathways programmed by small RNAs. *Science*, 296:1265–1269, 2002.

Received December 2002; revised June 2003.

E-mail address: tjacks@umich.edu